FINAL REPORT

Grant number: DE-FC26-05NT42631
Recipient: University of Kentucky Research Foundation (Center for Applied Energy Research)
Project title: Investigation of Aging Mechanisms in Lean NO_x Traps
Principal investigator: Mark Crocker

Date of report: June 25, 2010

DISCLAIMER

1. Executive summary

Lean NO_x traps (LNTs) represent a promising technology for the abatement of NO_x under lean conditions. Although LNTs are starting to find commercial application, the issue of catalyst durability remains problematic. LNT susceptibility to sulfur poisoning is the single most important factor determining effective catalyst lifetime. The NO_x storage element of the catalyst has a greater affinity for SO_3 than it does for NO_2, and the resulting sulfate is more stable than the stored nitrate. Although this sulfate can be removed from the catalyst by means of high temperature treatment under rich conditions, the required conditions give rise to deactivation mechanisms such as precious metal sintering, total surface area loss, and solid state reactions between the various oxides present. The principle objective of this project was to improve understanding of the mechanisms of lean NO_x trap aging, and to understand the effect of washcoat composition on catalyst aging characteristics.

The approach utilized involved detailed characterization of model catalysts prior to and after aging, in tandem with measurement of catalyst performance in NO_x storage and reduction. In this manner, NO_x storage and reduction characteristics were correlated with the evolution of catalyst physico-chemical properties upon aging. Rather than using poorly characterized proprietary catalysts, or simple model catalysts of the $Pt/BaO/Al_2O_3$ type (representing the first generation of LNTs), $Pt/Rh/BaO/Al_2O_3$ catalysts were employed which also incorporated CeO_2 or CeO_2-ZrO_2, representing a model system which more accurately reflects current LNT formulations. Catalysts were prepared in which the concentration of each of the main components was systematically varied: Pt (50, 75 or 100 g/ft^3), Rh (10 or 20 g/ft^3), BaO (15, 30 or 45 g/L), and either CeO_2 (0, 50 or 100 g/L) or CeO_2-ZrO_2 (0, 50 or 100 g/L). A high surface area La-stabilized alumina was used to support the BaO phase. Catalysts were obtained by washcoating onto standard cordierite substrates, the total washcoat loading being set at 260 g/L. La-stabilized alumina was used as the balance. Subsequent to de-greening, the NOx storage and reduction characteristics of the catalysts were evaluated on a bench reactor, after which the catalysts were aged on a bench reactor to the equivalent of *ca*. 75,000 miles of road aging using a published accelerated aging protocol. The aged catalysts were then subjected to the same evaluation proecdure used for the de-greened catalysts. In addition to the use of standard physico-chemical analytical techniques for studying the fresh and aged model catalysts, use was made of advanced analytical tools for characterizing their NO_x storage/reduction and sulfation/desulfation characteristics, such as Spatially resolved capillary-inlet Mass Spectrometry (SpaciMS) and *in situ* Diffuse Reflectance Infrared Fourier Transform Spectroscopy (DRIFTS).

From these studies, several key findings emerge with respect to the mechanisms of LNT catalyst aging:

- Steady state and lean-rich cycling data acquired for aged model LNT catalysts indicate that the decline in cycle averaged NO_x conversion after aging can be attributed to deterioration of three key catalyst functions, *viz*., NO_x storage, NO_x release and NO_x reduction.
- High resolution transmission electron microscopy data reveal the occurrence of significant Pt sintering on the BaO/Al_2O_3 washcoat component after LNT aging, whereas Pt supported on CeO_2 is sintered to a lesser degree.

- Analytical data (XPS, XRD and TEM/EDS/EELS) reveal that sulfur accumulates in the washcoat as $BaSO_4$ over the course of repeated sulfation-desulfation cycles. Sulfur accumulation on CeO_2 is not observed.
- Based on the analytical data, LNT degradation is attributed to two main factors: (i) Pt sintering (along with possible Ba phase aggregation), resulting in Pt-Ba phase segregation, and (ii) sulfation of the Ba NO_x storage material (which degrades NO_x storage capacity).

Of particular significance is the spectacular improvement in LNT durability which can be achieved through the incorporation of CeO_2 or CeO_2-ZrO_2 (particularly the latter). This improvement is attributed to three main factors, *viz.*:

- Ceria can be directly involved in NO_x storage/reduction as a supplement to the main NO_x storage component (Ba); hence, even if the NO_x storage capacity of the Pt/Ba/Al_2O_3 component is degraded as a result of aging, NO_x storage can still proceed on the Pt/CeO_2(-ZrO_2) component. Similarly, the Pt/CeO_2(-ZrO_2) component can contribute to NO_x reduction.
- Unlike the Pt/Ba/Al_2O_3 component, for which segregation of the Pt and Ba can occur during aging, migration and sintering of Pt in the Pt/CeO_2(-ZrO_2) component does not lead to the same degree of segregation, i.e., the Pt and CeO_2(-ZrO_2) remain in intimate contact, which should be beneficial for the retention of NO_x storage efficiency, as well as efficient nitrate decomposition.
- Ceria-containing catalysts exhibit superior sulfation and desulfation characteristics as compared to their non-ceria analogs; more particularly, the ability of ceria to trap sulfur results in decreased sulfur accumulation on the main Ba NO_x storage component. Further, the ceria can be completely desulfated, unlike the Ba phase on which sulfur accumulation is observed over the course of repeated sulfation-desulfation cycles.

Overall, this study provides new insights into the factors responsible for the degradation of LNT performance upon extended use. Furthermore, the spectacular improvement in LNT durability which can be achieved through the incorporation of CeO_2 or CeO_2-ZrO_2 serves to highlight the important role that ceria serves in LNT catalysts. From this it follows that in order to develop accurate microkinetic models for real world LNT catalysts, it will be necessary to fully consider the contribution of the ceria component to the catalytic chemistry taking place.

2. Accomplishments with respect to project goals and objectives

2.1 Goals and objectives

The goal of this project was to deepen understanding of the mechanisms of lean NO_x trap aging. Within this broad aim, and in accordance with the technical priorities of the CLEERS Lean NO_x Trap Focus Group, the following specific objectives were set at the beginning of the project:

(i) The effect of washcoat composition on catalyst aging characteristics will be examined. $Pt/Rh/CeO_2(\text{-}ZrO_2)/BaO/Al_2O_3$ catalysts will be prepared with systematic variation of the concentration of the four main (active) components (Pt, Rh, CeO_2-ZrO_2 mixed oxide and BaO supported on alumina), and aged on a synthetic gas bench. The physical and chemical properties of the fresh and aged catalysts will be characterized, including:

- catalyst performance in NO_x, CO and HC conversion (measured over repeated lean-rich cycles)
- NO_x adsorption capacity under lean conditions
- sulfur retention, i.e., degree of formation of non-regenerable sulfur
- washcoat micro-structure (as reflected in surface area and porosimetry measurements, and characterization using electron microscopy)
- extent of contact between precious metal particles and NO_x storage materials
- precious metal sintering.

(ii) SpaciMS will be applied to the analysis of transient phenomena in the degreened and aged catalysts. Specifically, NO_x, O_2, H_2 and CO_2 profiles will be monitored along the length of the catalyst; oxygen profiles will provide information about lean-to-rich and rich-to-lean transition timing with spatial resolution, and CO_2 profiles about CO consumption. Additionally, by applying chemical ionization mass spectrometry for the simultaneous analysis of different sulfur species, the kinetics and mechanism of catalyst desulfation will be studied. Specific reactions/processes to be examined comprise:

- NO_x storage under lean conditions
- Reduction of NO_x under rich conditions
- Conversion of H_2, CO and hydrocarbon species during rich conditions and lean-rich transients
- Formation of NH_3 during rich conditions
- Release of SO_2, SO_3, COS and H_2S during desulfation.

Additionally, based on the data acquired using SpaciMS, catalyst performance will be correlated with residual (non-regenerable) sulfur concentration along the length of the catalyst.

2.2 Accomplishments

(i) The effect of washcoat composition on catalyst aging characteristics:

- Model monolithic $Pt/Rh/BaO/Al_2O_3$ catalysts were prepared which also incorporated CeO_2 or CeO_2-ZrO_2, and in which the concentrations of Pt, Rh, BaO and CeO_2 were systemically varied. Two simple powder catalysts were also prepared, corresponding to (i) $Pt/BaO/Al_2O_3$ and (ii) a physical mixture of $Pt/BaO/Al_2O_3$ mixed with Pt/CeO_2.

- Steady state and lean-rich cycling data acquired for aged model LNT catalysts indicated that the decline in cycle averaged NO_x conversion after aging can be attributed to deterioration of three key catalyst functions, *viz*., NO_x storage, NO_x release and NO_x reduction.
- HRTEM data revealed the occurrence of significant Pt sintering on Al_2O_3 after LNT aging, whereas Pt supported on CeO_2 sintered to a lesser degree.
- XPS, XRD and TEM/EDS/EELS data revealed that sulfur accumulates in the washcoat as $BaSO_4$ over the course of repeated sulfation-desulfation cycles. Sulfur accumulation on CeO_2 is not observed.
- Based on the analytical data, LNT degradation is attributed to two main factors: (i) Pt sintering, resulting in Pt-Ba phase segregation, and (ii) sulfation of the Ba NO_x storage material (which degrades NO_x storage capacity).
- Spectacular improvement in LNT durability is observed for catalysts containing CeO_2 or CeO_2-ZrO_2 relative to their non-ceria containing analog. This is attributed to (i) the ability of ceria to participate in NO_x storage/reduction as a supplement to the main Ba NO_x storage component; (ii) the fact that Pt and CeO_2(-ZrO_2) are not subject to the same degree of phase segregation as Pt and Ba; and (iii) the ability of ceria to trap sulfur, resulting in decreased sulfur accumulation on the Ba component.

(ii) Study of transient phenomena in degreened and aged catalysts:

- NOx storage experiments performed on powder model catalysts showed that the addition of ceria is beneficial with respect to NOx storage at low temperatures (up to 300 °C). In lean-rich cycling experiments, the presence of ceria was found to be beneficial at all temperatures in the range 200-400 °C. This is attributed to the superior rich phase regeneration characteristics of the ceria-containing catalyst studied, which results in a higher effective NOx storage capacity during cycling.
- Lean-rich cycling experiments performed on model monolith LNT catalysts identified significant effects associated with the presence of ceria; these include increased NO_x storage (particularly at low temperatures), resulting in improved NO_x conversion levels, and superior selectivity to N_2 during reduction of stored NO_x (at fixed reductant concentration).
- Transient response studies showed that the introduction of ceria into LNT catalysts results in increased water-gas shift activity. However, the use of high OSC ceria-based oxides can result in rapid depletion of the CO and H_2 reductants along the length of the catalyst, due to reaction with stored oxygen. This finding underscores the need to balance the oxygen storage capacity in LNT catalysts.
- The addition of ceria to Ba-based LNT catalysts exerts a positive effect on LNT performance in the presence of sulfur. DRIFTS and NO_x storage capacity measurements indicate that ceria is able to store sulfur and thereby mitigate sulfation of the main (Ba) NO_x storage phase.
- Desulfation of a ceria-containing model catalyst was found to occur in two stages, corresponding to sulfur elimination from the ceria phase at ~450°C, followed by sulfur loss from the Ba phase at ~650°C. Significantly, the ceria-containing catalyst displayed relatively lower sulfur evolution from the Ba phase than its non-ceria analog, confirming that the presence of ceria lessened the degree of sulfur accumulation on the Ba phase. In

addition, desulfation experiments revealed the importance of maintaining the Pt and Ba phases in close contact for efficient LNT desulfation

- Bench reactor experiments confirmed that the presence of ceria is beneficial for lowering the required desulfation temperature of barium-based LNT catalysts; the precious metal loading is also indicated to be of importance.

3. Summary of project activities

3.1 Preparation of model catalysts

Rather than using poorly characterized proprietary catalysts, or simple model catalysts of the $Pt/BaO/Al_2O_3$ type (representing the first generation of LNTs), in this study we elected to employ $Pt/Rh/BaO/Al_2O_3$ catalysts which also incorporate CeO_2 or CeO_2-ZrO_2, representing a model system which more accurately reflects current LNT formulations. Catalysts were prepared in which the concentrations of each of the main components were systematically varied: Pt (50, 75 or 100 g/ft^3), Rh (10 or 20 g/ft^3), BaO (15, 30 or 45 g/L), and either CeO_2 (0, 50 or 100 g/L) or CeO_2-ZrO_2 (0, 50 or 100 g/L) (see Table 1). Catalysts were obtained by washcoating onto standard cordierite substrates, the total washcoat loading being set at 280 g/L. La-stabilized alumina was used as the balance.

Table 1. Model monolithic catalysts prepared in this work

Catalyst code	**Component loading[a]**					
	Pt, g/L (g/cuft)	Rh, g/L (g/cuft)	BaO, g/L	CeO_2[b], g/L	$Ce_{0.7}Zr_{0.3}O_2$, g/L	Al_2O_3[c], g/L
30-0	3.53 (100)	0.71 (20)	30	0	0	Balance
30-50	3.53 (100)	0.71 (20)	30	50	0	Balance
30-100	3.53 (100)	0.71 (20)	30	100	0	Balance
30-50Z	3.53 (100)	0.71 (20)	30	0	50	Balance
30-100Z	3.53 (100)	0.71 (20)	30	0	100	Balance
45-0	3.53 (100)	0.71 (20)	45	0	0	Balance
45-50	3.53 (100)	0.71 (20)	45	50	0	Balance
45-100	3.53 (100)	0.71 (20)	45	100	0	Balance
Pt-50	1.77 (50)	0.35 (10)	30	50	0	Balance
Pt-75	2.65 (75)	0.35 (10)	30	50	0	Balance
Pt-100	3.53 (100)	0.35 (10)	30	50	0	Balance

[a] Nominal loadings. Total washcoat loading = 260 g/L.
[b] Stabilized with 5 wt% La_2O_3.
[c] Stabilized with 3 wt% La_2O_3.

In addition, to facilitate the use of DRIFTS for *in situ* spectroscopic studies, two powder model catalysts were prepared:

1) 1 wt% Pt / 20 wt% BaO / Al_2O_3 (denoted hereafter as "PBA")
2) 1 wt% Pt / 20 wt% BaO / Al_2O_3 (74 wt%) + 1 wt% Pt / CeO_2 (26 wt%), physical mixture (denoted as "PBAC")

The $BaO:CeO_2$ ratio in catalyst PBAC was chosen so as to correspond to the ratio used in a number of the monolithic model catalysts prepared.

3.2 Effect of ceria addition on LNT NOx storage and regeneration behavior

As part of a broader study of catalyst composition-activity trends, the effect of ceria on LNT NOx storage and regeneration characteristics was examined. Representative results are shown in Figure 1, which compares NOx storage for the two powder model catalysts, PBA and PBAC. As shown, both catalysts exhibit their highest NOx storage capacity at 300 °C; for PBA the value is 0.27 mmol/g, the corresponding value for PBAC being 0.28 mmol/g. Compared to PBA, PBAC showed higher NOx storage capacity at 200 °C (0.24 vs 0.19 mmol/g), clearly showing that the addition of ceria is beneficial with respect to NOx storage at low temperature. In contrast, at 400 °C the storage capacity of PBA is greater than that of PBAC, indicating that ceria does not contribute substantially to NOx storage at this temperature. This was confirmed independently by DRIFTS measurements, thermal decomposition of surface nitrate species on ceria being complete by 400 °C.

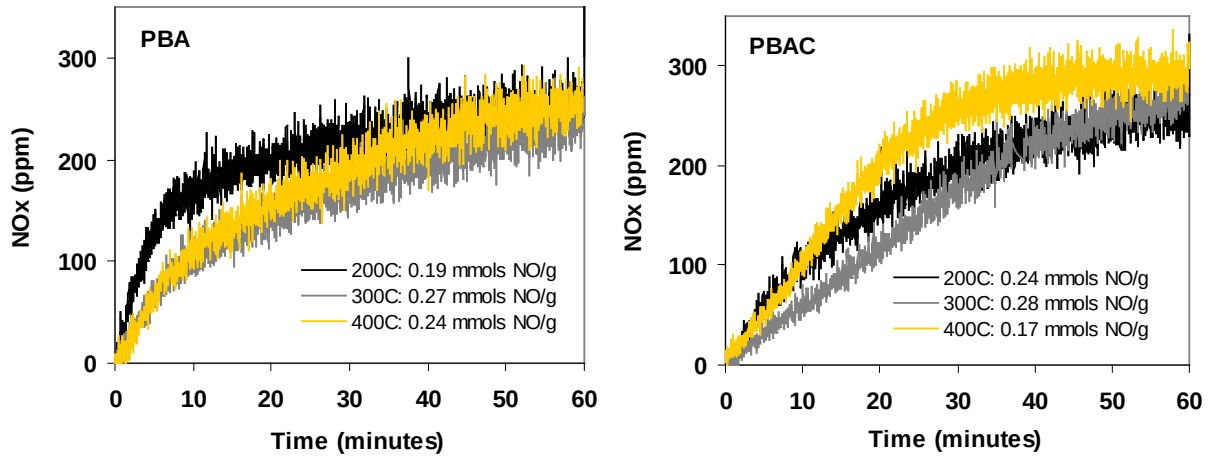

Figure 1. Outlet NOx concentration as a function of time during storage capacity measurement. Both catalysts were first reduced in a H_2/Ar flow at 450°C. NOx storage measurements were performed using a gas mixture consisting of 300 ppm NO, 8%O_2, 5%CO_2 and 5% H_2O.

Catalyst behavior was also examined under cycling conditions, using 6 min lean and 0.5 min rich times. Figure 2 shows the outlet NOx concentration profiles with time during the lean phase (T = 300 °C). The superior performance of catalyst PBAC is evident from the considerably lower NOx slip as compared to PBA, resulting in higher NOx conversion (averaged over lean-rich cycles). This was also found to be the case at 200 and 400 °C. Given the lower NOx storage capacity of PBAC at 400 °C, its superior NOx conversion at this temperature must derive from either lower emissions of unconverted NOx during the rich phase, or a more extensive regeneration during the rich phase which results in a higher effective NOx storage capacity. The former explanation can be excluded based on an analysis of the reactor effluent, both catalysts showing near zero NOx emissions during the rich phase. Further, *in situ* DRIFTS studies provide support for the superior regeneration characteristics of catalyst PBAC. Figure 3 shows the results of experiments in which the two catalysts were loaded with NOx and then subjected to H_2-TPR. According to DRIFT spectra, nitrate species on PBAC are removed at a slightly lower

temperature than those on PBA, as reflected in the decrease in intensity of the nitrate bands at 1415 and 1330 cm^{-1}. This effect is attributed to the ability of ceria to store NOx, thereby lessening the amount of bulk barium nitrate formed (this being the most difficult form of nitrate to reduce).

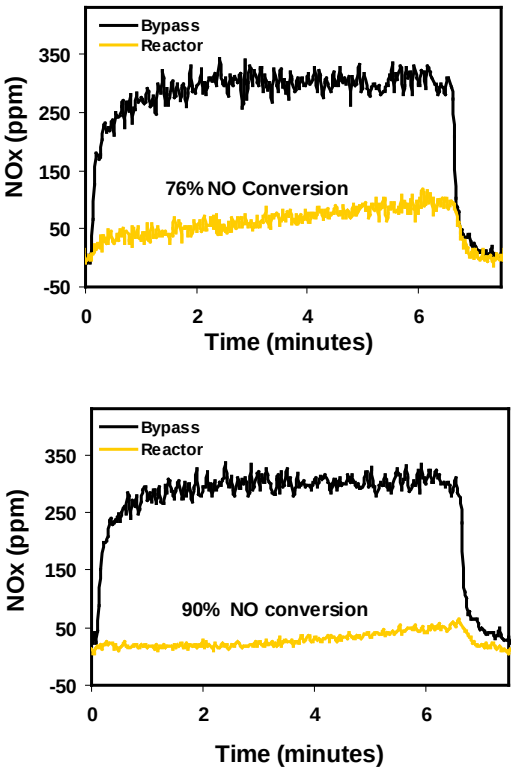

Figure 2. Outlet NOx concentration as a function of time during steady state lean-rich cycling. Top: catalyst PBA; bottom: catalyst PBAC. Conditions: 30 s rich: 3375 ppm H_2, 5625 ppm CO, 5% CO_2, 5% H_2O; 6 min lean: 300 ppm NO, 8% O_2, 5% CO_2, 5% H_2O.

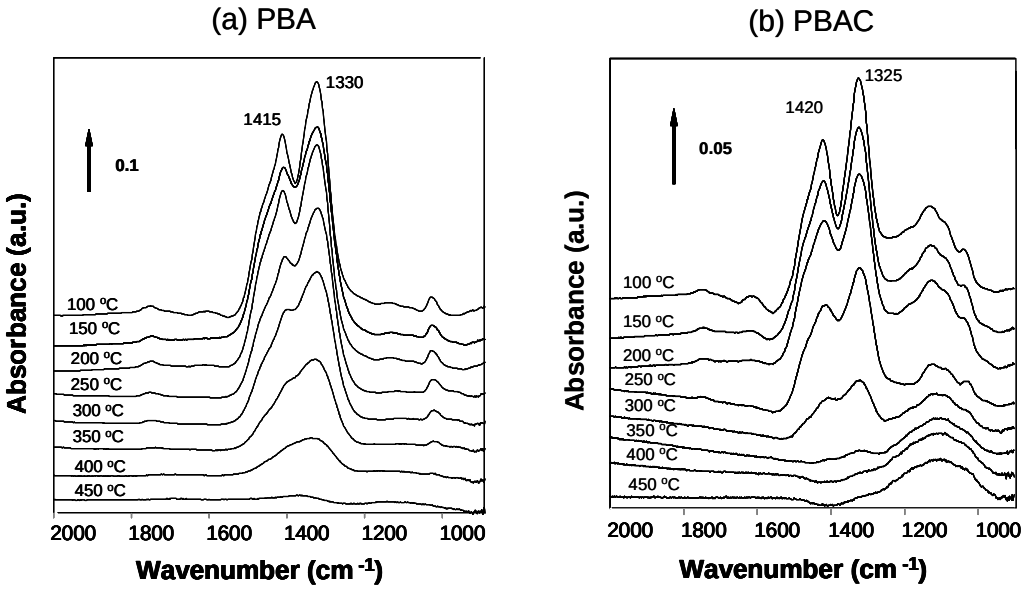

Figure 3. DRIFT spectra of catalysts PBA and PBAC loaded with NOx during H_2-TPR.

3.3 Composition-activity relationships in model lean NO_x trap catalysts

The NO_x storage and release properties of a series of fresh (degreened) model monolith catalysts were assessed on a bench reactor under steady state cycling conditions in the range 150-450 °C. In order to illustrate the effect of ceria content on catalyst performance, results for four catalysts are compared in Figure 4, *viz.*: catalyst 30-0 (containing 30 g BaO and 0 g CeO_2 per liter of catalyst), 30-50 (30 g BaO/L and 50 g CeO_2/L), 30-100 (30 g BaO/L and 100 g CeO_2/L) and 30-100Z (containing 30 g BaO/L and 100 g CeO_2-ZrO_2/L, the latter corresponding to 70 mol% CeO_2 and 30 mol% ZrO_2). In all cases the BaO was present as 21.4 wt% BaO supported on alumina, while fixed Pt and Rh loadings were used (3.5 g/L and 0.7 g/L, respectively).

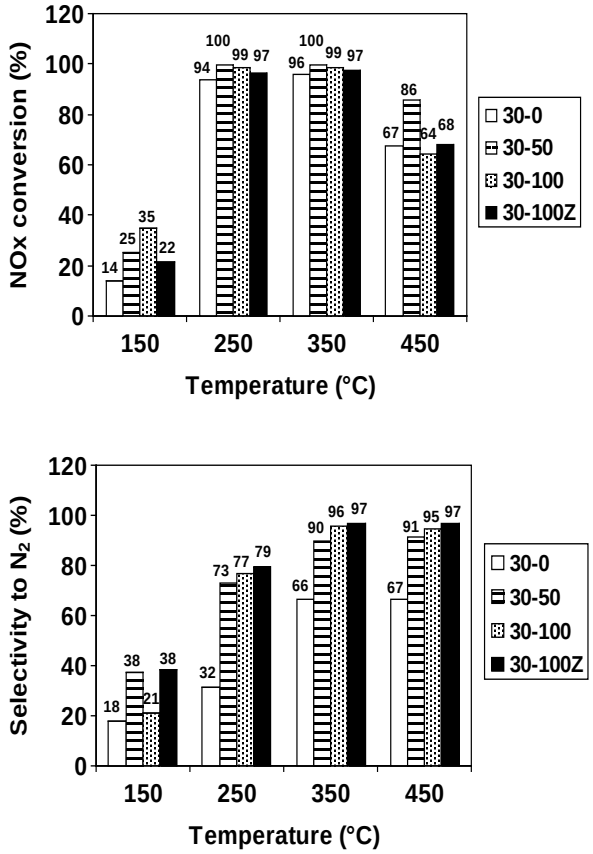

Figure 4. Cycle averaged NOx conversion (top) and selectivity to N_2 (bottom). Conditions: lean (60 s): 300 ppm NOx, 10% O_2, 5% CO_2, 5% H_2O; rich (5 s): 1.575% H_2, 2.625% CO, 5% CO_2, 5% H_2O, with N_2 as balance, GHSV = 30,000 h^{-1}

From the data collected, several trends emerge:

(i) Under the cycling conditions employed (60 s lean/5 s rich), NO_x storage efficiency in the temperature range 150-350 °C was improved upon addition of ceria to the base $Pt/Rh/BaO/Al_2O_3$ formulation. At 150 °C each of the catalysts displayed lean phase NO_2 slip, indicating that NO oxidation was not rate limiting; rather, NO_x storage at this temperature appears to be limited by the inability to remove nitrates and nitrites during the regeneration phase.

(ii) High rich phase NO_x slip was observed for all of the catalysts at 150 °C, resulting from an imbalance in the rates of nitrate decomposition and NO_x reduction. Although the ceria-containing catalysts showed increased NO_x slip during the regeneration phase, the overall NO_x

conversion increased with ceria loading at 150 °C. Further, the presence of ceria was found to be beneficial for NO_x conversion across the temperature range 150-350 °C.

(iii) N_2O was the major NO_x reduction product at 150 °C over all of the catalysts, although low NO_x conversion levels limited the N_2O yield. At higher temperatures N_2 was the main product of NO_x reduction, although NH_3 formation was also observed. Selectivity to NH_3 decreased with increasing ceria loading, which is rationalized on the basis that NH_3, formed as a primary reduction product [1], is consumed by reaction with stored oxygen (and residual stored NO_x) as the reaction front propagates along the length of the catalyst.

3.4 Effect of ceria loading on intra-catalyst H_2 concentration during rich purging

Ceria has the ability to both catalyze the production of H_2 in situ via the water-gas shift reaction ($CO + H_2O \rightarrow H_2 + CO_2$), and contribute to the consumption of reductants via their reaction with stored oxygen. In order to better understand this apparent trade-off, intra-catalyst hydrogen concentrations were determined during NO_x reduction using SpaciMS. Figure 5 (see next page) shows the results obtained for catalysts 30-0, 30-100 and 30-100Z under steady state NO_x storage-reduction cycling at 350 °C, the H_2 concentrations being measured at (i) the catalyst inlet ("In Cat"), (ii) one quarter of the way along the catalyst length ("0.25 Cat"), (iii) halfway along the catalyst length ("0.5 Cat"), and (iv) at the catalyst outlet ("Out Cat").

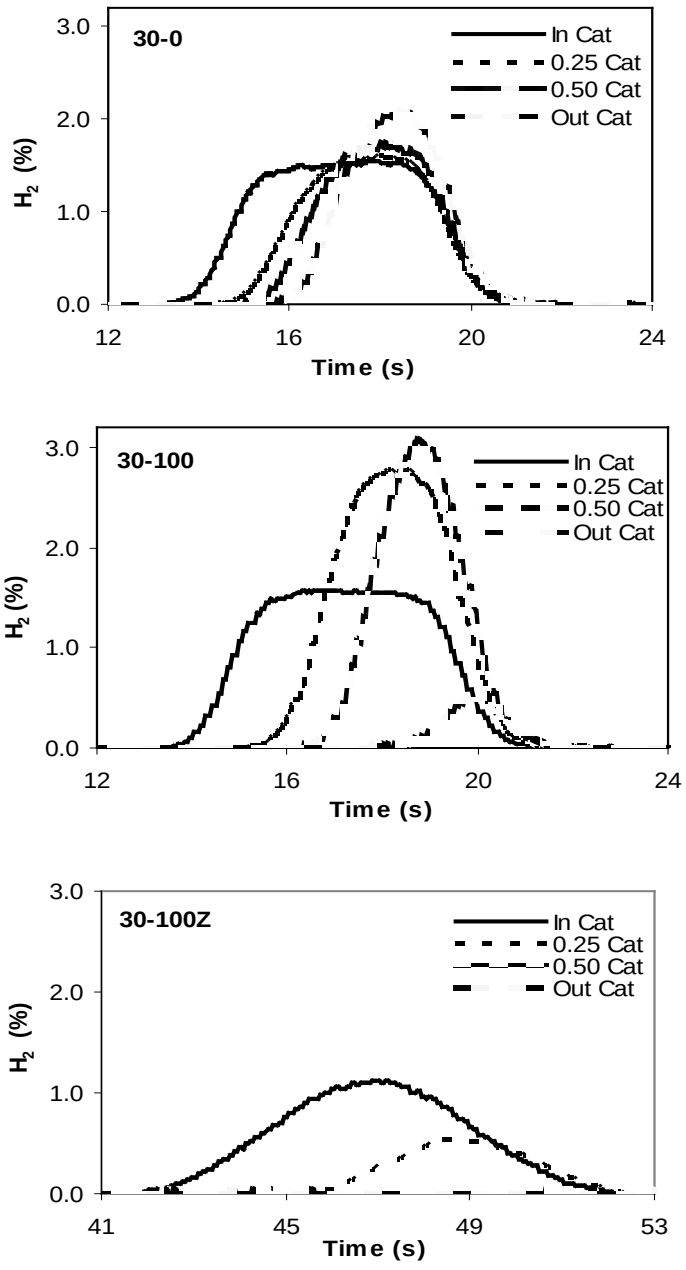

Figure 5. H_2 concentration profiles measured along catalyst length during rich purge (T = 350°C)

For catalyst 30-0, a slight increase in the H_2 concentration is observed along the length of the catalyst during rich phase operation, resulting from the water-gas shift reaction. In the case of 30-100, high concentrations of H_2 (up to 3%) are measured at the positions one-quarter and halfway into the catalyst (from the inlet), indicative of high water-gas shift activity. This can be attributed to the presence of the Pt/CeO_2 component, which is known to be a highly active catalyst for this reaction. However, the H_2 concentration measured at the catalyst outlet is very low (<0.5%), suggesting that the H_2 formed is subsequently consumed by reaction with oxygen stored in the rear of the catalyst. It can be inferred that towards the rear of the catalyst most of the CO in the feed gas has been consumed, such that the rate of H_2 production from the water-gas shift reaction no longer exceeds the rate of H_2 consumption. FT-IR data are consistent with

this notion; as shown in Figure 6, for catalyst 30-50 the rich phase outlet CO concentration measured during lean-rich cycling does not exceed 0.1% (as compared to the inlet CO concentration of 2.625%), while that for catalyst 30-100 is even lower (maximum of 132 ppm).

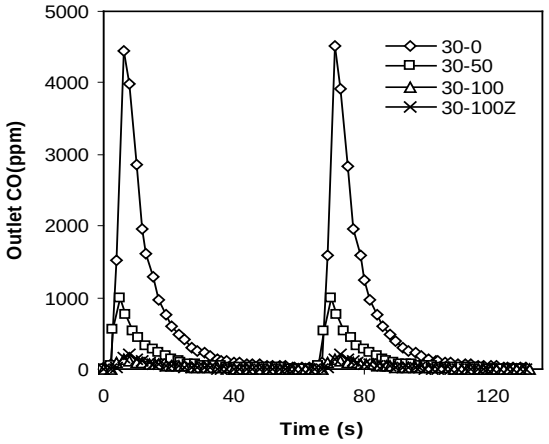

Figure 6. Outlet CO concentration measured during rich purge (T = 350°C).

For catalyst 30-100Z very different behavior is observed, resulting from the high OSC of the ceria-zirconia component. The H_2 concentration in the catalyst falls off rapidly from the inlet value (Figure 5), such that no H_2 is detected at the mid-point or in the rear of the catalyst. Coupled with this, the CO concentration measured at the catalyst outlet is found to be near zero for the duration of the rich purge (Figure 6), consistent with rapid depletion of the CO and H_2 reductants via reaction with stored oxygen. This result underscores the need to balance the oxygen storage capacity in LNT catalysts [2].

3.5 Effect of catalyst composition on LNT sulfation and desulfation characteristics

In order to study the influence of ceria on LNT sulfation and desulfation characteristics, two Ba-based model catalysts were used, of which one contained ceria. The composition of the catalysts corresponded to i) 1 wt% Pt / 20 wt% BaO / Al_2O_3 (PBA); and ii) 1 wt% Pt / 20 wt% BaO / Al_2O_3 (74 wt%) + 1 wt% Pt / CeO_2 (26 wt%), physical mixture (PBAC). Figure 7 shows a series of DRIFT spectra acquired during exposure of PBA and PBAC to feed gas containing 300 ppm NO, 10% O_2, 5 % H_2O and 27 ppm SO_2. In the case of PBA, bands grow in at 1420 and 1320 cm^{-1} which can be attributed to Ba nitrate species [3], while an intense band at 1122 cm^{-1} corresponds to a surface Ba sulfate species. A weaker band at 978 cm^{-1} can be assigned to surface $Al_2(SO_3)_3$. Based on the evolution of the spectra with time, it is apparent that at short reaction times (e.g., 5 min) the nitrates are the dominant surface species, reflecting the higher concentration of NO in the feed relative to SO_2. However, beyond this point the sulfate bands become progressively more intense, while the intensities of the nitrate bands are slightly decreased. This observation is consistent with strong adsorption of SO_x on the catalyst, which effectively competes with NO_x for storage sites.

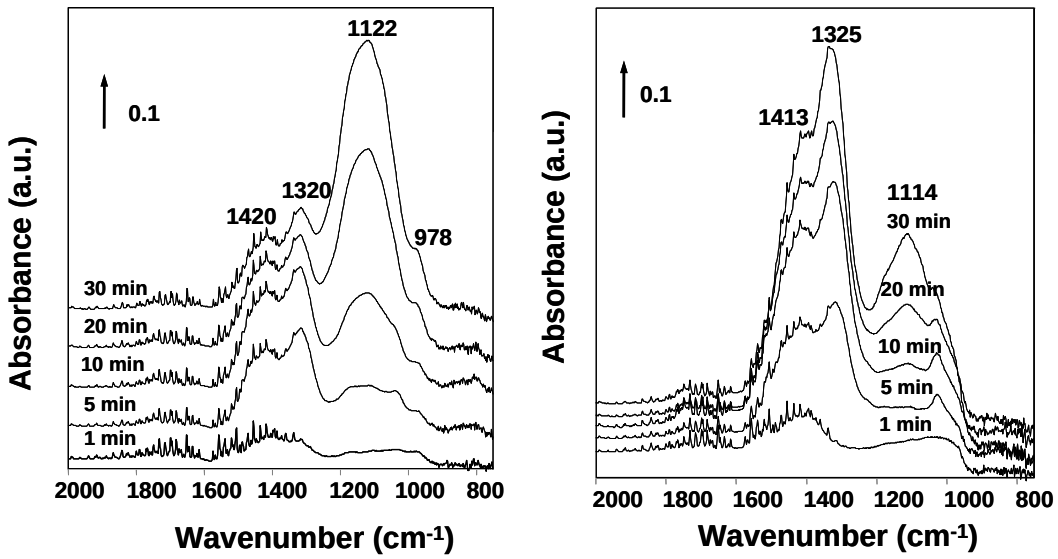

Figure 7. DRIFT spectra obtained upon exposure of PBA (left) and PBAC (right) to $SO_2/NO/O_2/H_2O$.

In the case of the ceria-containing catalyst, PBAC, rather different behavior is observed. After 5 min of exposure to the feed gas, the spectrum is again dominated by the presence of Ba nitrate bands, while a shoulder at *ca*. 1510 cm^{-1} is indicative of the formation of a nitrate species on ceria [4]. At longer reaction times the Ba nitrate bands continue to increase in intensity, while a band due to Ba sulfate grows in at 1114 cm^{-1}. Even at the end of the experiment (30 min duration), the sulfate band intensity remains substantially less than that of the Ba nitrate bands. These observations suggest that nitrate and sulfate were able to form at different sites on the catalyst.

In order to provide additional insight into their desulfation behavior, temperature-programmed reduction (TPR) experiments were performed on sulfated samples of PBA and PBAC (Figure 8). During H_2-TPR sulfur was released from both catalysts mainly as H_2S; release of H_2S occurred at ~650 °C from PBA, whereas PBAC showed two discrete H_2S release events at ~450 °C and ~650 °C. From this it follows that the H_2S release at ~450 °C corresponds to desulfation of the ceria phase (confirmed by reference experiments), with Ba desulfation occurring at the higher temperature. Significantly, PBAC displayed relatively lower H_2S evolution from the Ba phase than PBA, confirming that the presence of ceria in PBAC lessened the degree of sulfur accumulation on the Ba phase.

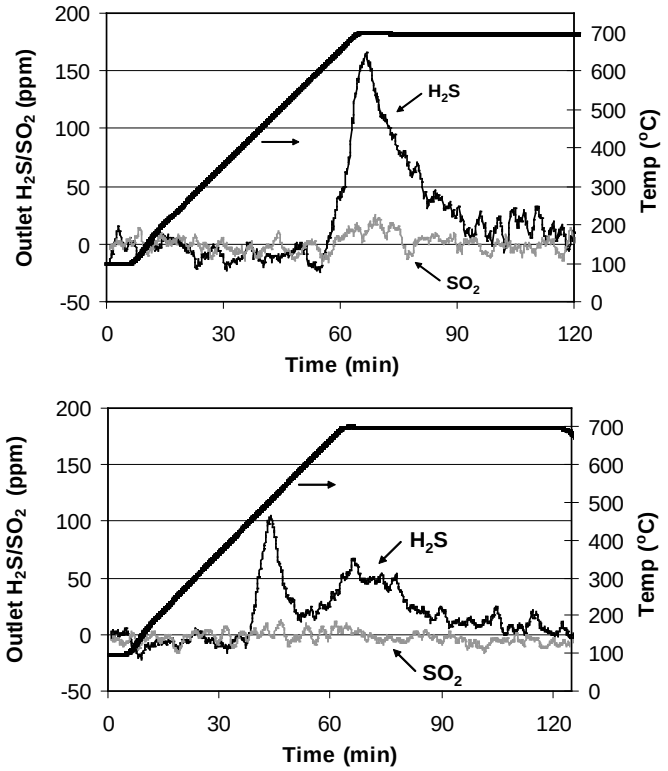

Figure 8. Sulfur release from PBA (top) and PBAC (bottom) during temperature programmed desulfation (1% H_2, 5% H_2O, 5% CO_2 in Ar).

TPR experiments were also performed with the aim of ascertaining the effect of Pt location on the sulfation and desulfation behavior of Ba-based LNT formulations. For this purpose, a simple physical mixture of 1 wt% Pt/Al_2O_3 and 20 wt% BaO/Al_2O_3 (1:1 weight ratio) was used. As shown in Figure 9, two main sulfur desorption events are observed. The first corresponds to sulfur release from the alumina phase (370 °C, confirmed by reference experiments), while the second maximum is extremely broad and spans the range 725-775 °C. Comparing these results with those obtained for PBA at the same sulfur loading, it is apparent that physical separation of the Pt and Ba phases results in increased sulfur storage on the alumina, presumably as a consequence of SO_3 spillover from Pt to the alumina support during sulfation. Additionally, the desulfation temperature of the $BaSO_4$ is shifted by 20-40 °C towards higher temperature, i.e., towards the position characteristic of bulk $BaSO_4$ [5]. This is in keeping with the idea that decomposition of surface $BaSO_4$ is facilitated by H ad-atoms which spill over from the Pt sites onto the sulfated Ba phase. Physical separation of the Pt and Ba phases appears to inhibit this process, with the consequence that the surface $BaSO_4$ behaves more like bulk $BaSO_4$ with respect to its desulfation properties. We note that somewhat analogous findings have been reported for nitrate decomposition on physical mixtures of Pt/Al_2O_3 and BaO/Al_2O_3 [6]: in the absence of hydrogen spillover from Pt to the Ba phase, considerably higher temperatures are required to achieve nitrate decomposition than is usual for $Pt/BaO/Al_2O_3$ catalysts.

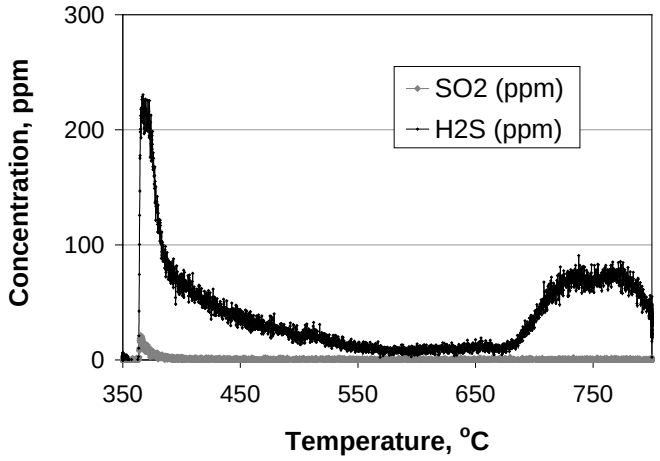

Figure 9. Sulfur release from 20 wt% BaO/Al_2O_3 + 1 wt% Pt/Al_2O_3 (1:1 physical mixture) during temperature programmed desulfation (1% H_2, 5% H_2O, 5% CO_2 in Ar).

3.6 NOx storage-reduction characteristics of LNT catalysts subjected to simulated road aging

In order to study the effect of washcoat composition on catalyst aging characteristics, core samples of the fully formulated monolithic catalysts were aged on a bench reactor using a cycle developed by Ford Motor Co. [7], designed to simulate road aging. Each cycle consisted of (i) sulfating the catalyst at 350 °C to an equivalent loading of 1 g S/L, (ii) desulfation at 700 °C for 10 min under cycling (5 s lean/15 s rich at λ= 0.90), and (iii) holding at 650 °C for 30 min under lean conditions (to simulate DPF regeneration). Together, these three conditions constituted one aging cycle. Each catalyst was aged for 50 cycles, which is estimated to be equivalent to *ca*. 75,000 miles of road aging. After aging, the catalysts were exposed to rich conditions at 750 °C for 10 min to remove residual sulfur and then evaluated on a bench reactor.

Representative cycle averaged NO_x conversion and N_2 selectivity data for the aged catalysts are shown in Table 2, together with oxygen storage capacity (OSC) data obtained at 350 °C. For comparison purposes, data for the fresh (degreened) catalysts are included. Considering the NO_x conversion data, it is apparent that the performance of catalyst 30-0, containing no ceria, was severely degraded after aging. In comparison, catalyst 30-100, containing 100 g/L of ceria, continued to show high levels of NO_x conversion at 250-350 °C, while catalyst 30-100Z, containing 100 g/L of CeO_2-ZrO_2, retained the highest degree of activity; indeed, NO_x conversion levels for the aged catalyst were only slightly lower than for the fresh state. Analysis of data (not shown) pertaining to the lean phase NO_x storage efficiency and rich-phase NO_x release characteristics of the three catalysts indicates that the decreased NO_x conversion after aging mainly results from degradation of the lean-phase NO_x storage and rich-phase regeneration efficiency under cycling. Regarding the lean-phase performance, NO_2 slip was consistently observed for all of the catalysts (at all temperatures), indicating that NO oxidation is not the limiting factor; rather, it is the inability of the catalyst to store NO_2 that limits the NO_x storage efficiency (NSE). To provide further insights into the origin of the NSE degradation, the NSE measured during the first lean cycle after complete catalyst regeneration (the “first cycle NSE”)

was compared with the NSE measured under steady state cycling (Table 3). Catalyst 30-0 exhibited a large difference between the two NSE values, implying that its NO_x storage efficiency was significantly limited by its inability to be completely regenerated during rich purging. However, a small difference between these two NSE values for catalysts 30-100 and 30-100Z indicates that these two catalysts retained their good regeneration characteristics.

Table 2. Comparison of OSC, cycle averaged NO_x conversion and N_2 selectivity before and after catalyst aging

Catalyst	Temp. (°C)	OSC (mmol/L)		NO_x conversion (%)		N_2 selectivity (%)	
		Fresh	Aged	Fresh	Aged	Fresh	Aged
30-0	250	--	--	94.3	39.7	31.7	41.7
	350	10.8	6.2	95.9	40.0	66.4	23.5
30-100	250	--	--	98.7	87.7	76.8	57.8
	350	28.0	18.5	98.7	91.1	95.9	88.3
30-100Z	250	--	--	97.2	92.0	79.5	15.8
	350	36.6	34.1	98.0	93.4	97.0	89.2

Conditions: Lean: 300 ppm NO, 10% O_2, 5% CO_2, 5% H_2O in N_2 (60 s); Rich: 1.575% H_2, 2.625% CO, 5% CO_2, 5% H_2O in N_2 (5 s); GHSV = 30,000 h^{-1}. OSC was measured without lean-phase NO, while using 4.2% H_2 as reductant during the rich phase.

Table 3. Comparison of cycled averaged and first cycle NO_x storage efficiencies before and after catalyst aging

Catalyst	Temp. (°C)	Cycle av. NSE (%)		First cycle NSE (%)	
		Fresh	Aged	Fresh	Aged
30-0	250	94.7	38.0	98.8	84.4
	350	96.8	43.2	98.3	74.7
30-100	250	98.8	94.5	99.5	97.0
	350	99.6	92.8	99.4	95.5
30-100Z	250	97.0	93.4	99.2	98.2
	350	97.7	95.5	99.2	98.1

Conditions as for Table 2.

From Table 2 it is apparent that after aging, all of the catalysts showed decreased selectivity to N_2 during NO_x reduction, the selectivity to NH_3 being increased. Simultaneously, in each case the catalysts exhibited decreased OSC after aging. This suggests that the decreases in N_2 selectivity and OSC are related, an idea which can be rationalized on the basis that: 1) a decrease in stored oxygen should result in an increased reductant concentration in the gas front, favoring the formation of NH_3 over N_2; 2) less stored oxygen will be available in the rear of the catalyst to react with initially formed NH_3 to give N_2.

3.7 Effect of LNT aging on NO_x reduction activity

As detailed above, evaluation of the aged monolith catalysts on a bench reactor under lean-rich cycling conditions revealed the beneficial effects of ceria incorporation with respect to the NO_x reduction performance of the aged catalysts. However, the transient nature of lean-rich cycling experiments, coupled with the integral nature of the monolith core sample, results in complex

spatial and temporal concentration variations within the catalyst during these measurements. These variations make it difficult to directly relate the outlet gas composition to the chemistry taking place inside the catalyst. Steady flow experiments were therefore performed in an effort to avoid the difficulties associated with transient LNT behavior, the aim being to decouple the NO_x storage/release process from the reduction reactions. This was accomplished by flowing NO_x and reductant species simultaneously over the catalyst.

The results of one such experiment are summarized in Fig. 10, in which NO reduction with H_2 was examined over fresh and aged samples of catalysts 30-0 (containing 30 g BaO/L of catalyst and 0 g CeO_2/L) and 30-100Z (containing 30 g BaO/L of catalyst and 100 g CeO_2-ZrO_2/L). As shown, in the fresh state both catalysts show excellent NO reduction activity, achieving 100% conversion to reduction products (N_2, NH_3 and N_2O) at 225 °C. After aging, catalyst 30-100Z shows a slight decline in NO conversion in the temperature range 125-175 °C, whereas a significant decline is observed for 30-0 over the range 125-300 °C. Striking too is the fact that both catalysts show increased selectivity to NH_3 between 125 and 300 °C after aging (Fig. 10 b), which mirrors the result obtained under lean-rich cycling.

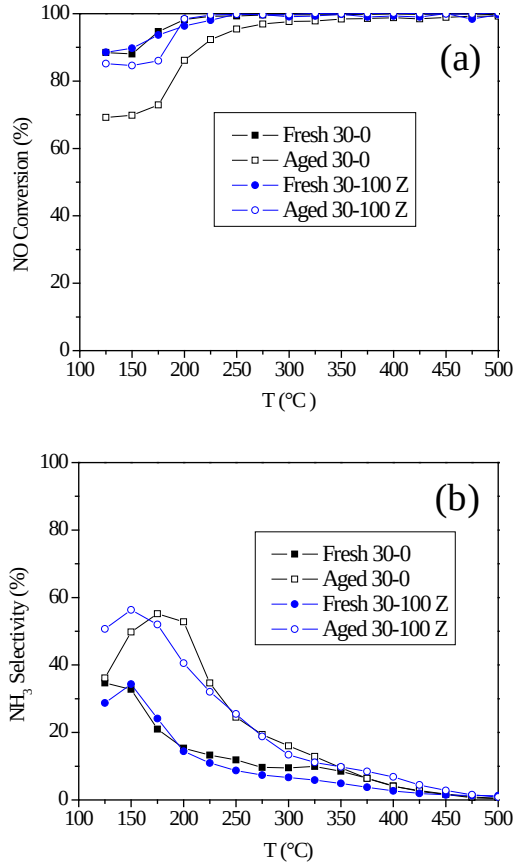

Figure 10. NO reduction with H_2 over fresh and aged catalysts 30-0 and 30-100Z: (a) NO conversion, (b) selectivity to NH_3. Reaction conditions: 300 ppm NO, 300 ppm H_2, 5% H_2O, 5% CO_2, balance N, GHSV = 120,000 h^{-1}.

It is generally agreed that the functioning of LNT catalysts involves four sequential steps [8]: (i) NO oxidation to NO_2, (ii) NO_x storage, (iii) NO_x release (i.e., nitrate decomposition) and (iv) NO_x reduction. As described in the foregoing section, under lean-rich cycling conditions it was found that simulated road aging resulted in significant deterioration of catalyst performance in

steps (ii) and (iii). For catalyst 30-0, containing no ceria, the decline in NO_x conversion after aging could be attributed mainly to the deterioration in cycle-averaged NO_x storage efficiency, which in turn is determined by the intrinsic NO_x storage efficiency (NSE) and the extent to which the catalyst is regenerated during rich purging. From the data show in Figure 10, it is apparent that for 30-0, catalyst activity for NO_x reduction is also compromised after aging (step iv). Indeed, this is consistent with increased rich phase NO_x release observed for 30-0 after aging, although we note that a decrease in the rate of the reverse spillover process (i.e., NO_x migration to Pt) due to Pt-Ba phase segregation could also contribute to the overall decrease in the rate of NO_x reduction (and hence increased rich phase NO_x slip).

3.8 Correlation of catalyst performance degradation with evolution of washcoat structure upon aging

Analytical data for the aged monolith catalysts reveal two main physico-chemical changes which can explain the degradation in LNT performance. First, residual sulfur was observed in the catalyst washcoats. According to XPS, TEM and XRD data, sulfur accumulated during the aging process as $BaSO_4$, thereby decreasing catalyst NO_x storage capacity. Second, sintering of the precious metals in the washcoat was inferred from H_2 chemisorption and TEM data, which can be expected to lessen the contact between the Ba and Pt phases, resulting in less efficient NO_x spillover from Pt to Ba during NO_x adsorption (and hence decreased NO_x storage efficiency). Similarly, decreased rich phase nitrate decomposition suggests that Pt-Ba phase segregation adversely affected the rate of reductant spillover from Pt to Ba.

These physico-chemical changes in the catalyst washcoats are readily apparent from HRTEM data. Figure 11, which shows TEM images of aged catalyst 30-0, illustrates the growth in Pt particle size that results from catalyst aging. In the fresh catalyst (not shown), Pt particles on Al_2O_3 surfaces display a narrow size range with the majority of particles ~2 nm in size, while Pt on Ba-rich surfaces show a broader size range from 1 to 4 nm. In contrast, Figure 11 reveals the presence of rather large Pt crystals, some as big as 25 nm. There is evidence that Pt particle growth occurred due to migration and coalescence as evidenced in Figure 11a, where Pt particles are shown that clearly have fused together. The EDS spectrum in Figure 11c shows that Ba and S occur together in the washcoat, consistent with sulfation of the Ba NO_x storage component.

Shown in Figure 12 are TEM images of aged catalyst 30-100 (containing 100 g/L of CeO_2). After aging, large (up to 30 nm) Pt particles are again present, although the majority of Pt particles are in a size range from 3 to 15 nm. Pt particles on CeO_2 have grown to a size of up to 5 nm, suggesting significantly less sintering of Pt on the ceria support in contrast to Al_2O_3 surfaces. There are also dense sulfur-rich Ba nodules present on the Al_2O_3 surface (Figure 12a). The EDS spot analysis in Figure 12b was performed at the area marked in Figure 12a and identified Ba, S, Al and Pt, pointing toward the fact that the $BaSO_4$ nodules were present on the surface of the Al_2O_3 support. The EELS spectrum taken over the entire sulfur-rich nodule clearly shows two sharp peaks for Ce M_5 M_4 and also for Ba M_5 M_4 (Figure 12c), as well as signals for O and Al (note that the signal for Al appears outside of the energy range depicted in Figure 12c). This suggests that the beam penetrated the ceria particles and also probed underlying BaO/Al_2O_3 particles. The EELS line scan results (Figure 12d) indicate that sulfur is only observed in the presence of barium, but does not occur where only ceria is located.

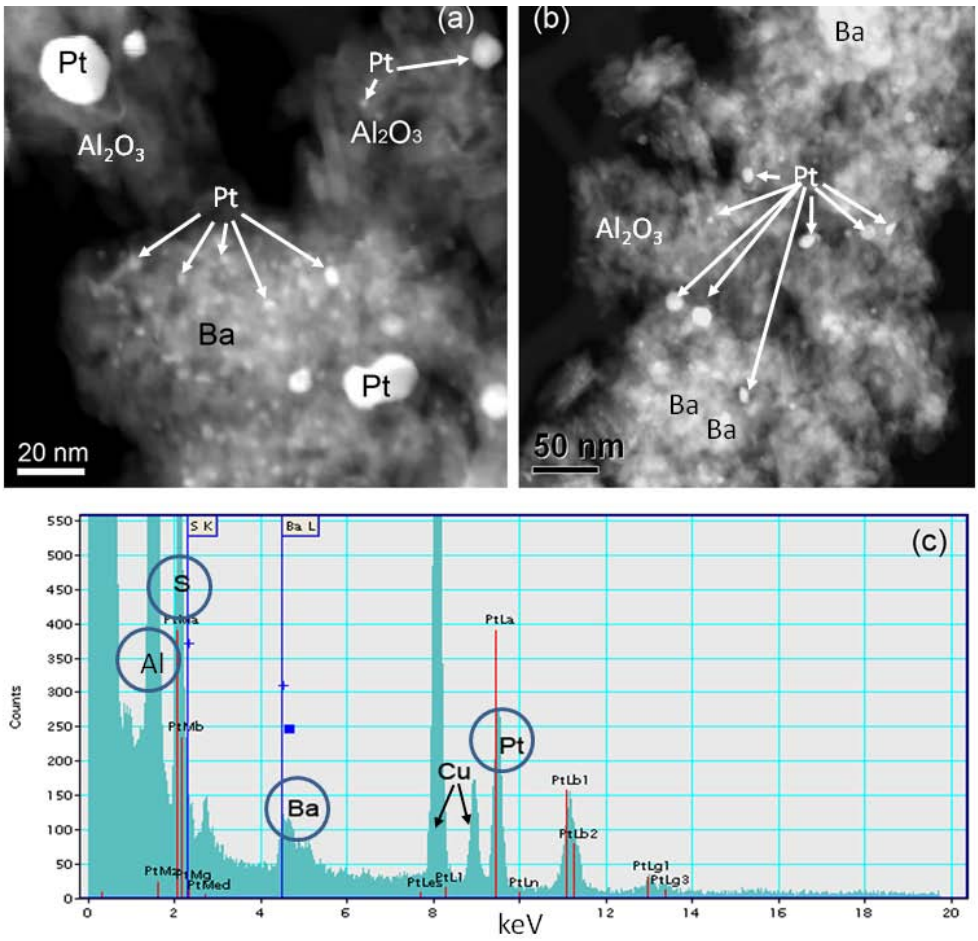

Figure 11. STEM images for aged 30-0 (a and b) illustrating large particle size range for Pt shown in white; (c) EDS spectrum.

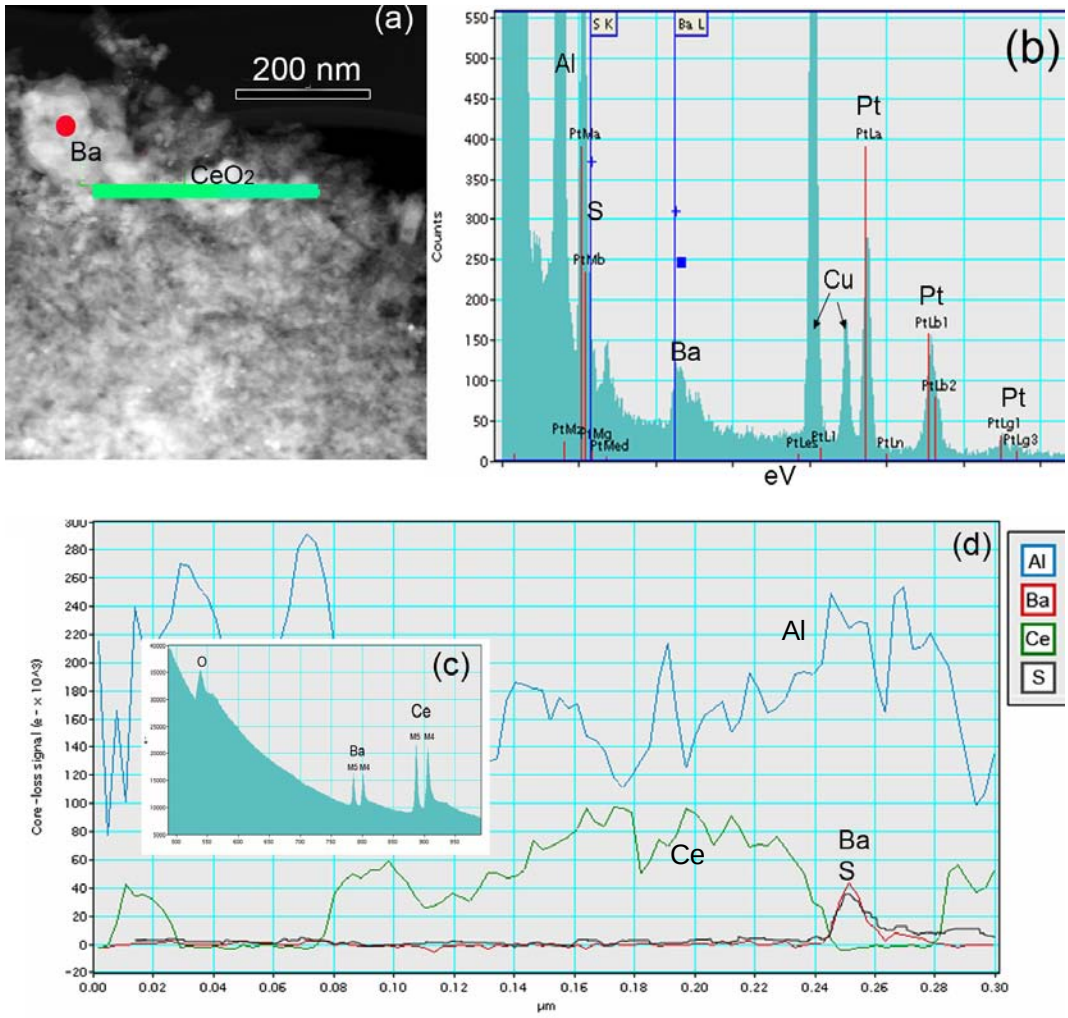

Figure 12. (a) STEM image for aged 30-100 showing Al_2O_3 support and Ba-rich nodules, as well as a CeO_2-rich area. The solid line indicates the EELS line scan region; (b) EDS spectrum recorded at the marked dotted area shown in (a); (c) EELS spectrum taken at the dotted area in (a); (d) EELS trace-line: the line is shown in (a). The trace line included 50 EELS measurements along the distance. S-enrichment is seen at the interface between Al_2O_3 and CeO_2.

Previous studies [9-15] have demonstrated the importance of the proximity of the Pt and Ba phases for efficient LNT functioning. Given that Pt is believed to act as a conduit for NOx spillover to and from the Ba phase, it follows that close proximity of Pt and Ba are required to achieve efficient NOx storage and reduction. The effect of Pt sintering on the Pt-Ba interface can be illustrated by consideration of the interfacial perimeter between Pt and its support (in this case BaO) at different levels of Pt dispersion. Assuming a hemispherical morphology for Pt particles, the relationship between the number of atoms in a Pt particle (N_{Pt}) and the particle size (d) is given by:

$$N_{Pt} = \frac{\frac{2}{3}\pi\left(\frac{d}{2}\right)^3 \sigma N a}{W a} \qquad (1)$$

where d is the particle diameter, σ is the density, *N*a is Avogadro's number, and W_a is the atomic weight. Based on face-centered cubic (fcc) packing for Pt, the number of surface atoms (N_{Pts}) as a function of particle size is given by:

$$N_{Pt_s} = 2\pi(d/2)^2\omega \quad (2)$$

where ω is the average atom density of Pt particle surface. Dispersion is defined as the percentage of surface atoms in the particle, i.e.:

$$\text{Dispersion} = N_{Pts}/N_{Pt} \quad (3)$$

From eqn. (1), it follows that the number of particles per gram of Pt (Σp) is given by:

$$\Sigma_p = \frac{3/2}{\pi(d/2)^3\sigma} \quad (4)$$

Assuming that the interfacial perimeter of a Pt particle corresponds directly to its circumference, the total interfacial perimeter per gram of Pt (λ_{Pt}) is obtained as follows:

$$\lambda_{Pt} = \pi * d * \Sigma p \quad (5)$$

As shown in Table 4 (see below), for a Pt dispersion of 40%, which is close to the values observed prior to aging for the monolithic catalysts in this work, the total perimeter of the Pt particles amounts to 6.22×10^{19} nm/g Pt. However, for a dispersion of 12%, which is typical of the values observed after aging, the total perimeter is only 5.6×10^{18}, i.e., a factor of eleven lower. These simple calculations are illustrative of the critical role that Pt particle size plays in determining the extent of Pt-Ba contact and, by implication, in governing LNT functioning. From this it follows that future attempts to predictively model the deactivation of LNT catalysts will have to incorporate the extent of Pt sintering as a key parameter.

Table 4. Total Pt-support interfacial perimeter as a function of Pt particle size, assuming hemispherical particle morphology

Av. Pt particle size (nm)	Dispersion	Number of atoms in particle	Number of particles/g Pt	Total interfacial perimeter (nm/g Pt)
1	100	18	17.80E+19	5.60E+20
2	59	139	2.22E+19	1.40E+20
3	40	468	6.60E+18	6.22E+19
4	30	1110	2.78E+18	3.50E+19
5	24	2167	1.42E+18	2.24E+19
8	15	8876	3.48E+17	8.76E+18
10	12	17336	1.78E+17	5.60E+18
20	6	138684	2.22E+16	1.40E+18

3.9 Effect of ceria on LNT durability

Overall, this study shows the spectacular improvement in LNT durability which can be achieved through the incorporation of CeO_2 or CeO_2-ZrO_2 (particularly the latter). Based on the foregoing, several factors are believed to be responsible for this improvement, *viz.*:

(i) Ceria can be directly involved in NO_x storage/reduction as a supplement to the main NO_x storage component (Ba); hence, even if the NO_x storage capacity of the Pt/Ba/Al_2O_3 component is degraded as a result of aging, NO_x storage can still proceed on the Pt/CeO_2(-ZrO_2) component. Similarly, the Pt/CeO_2(-ZrO_2) component can contribute to NO_x reduction.

(ii) Unlike the Pt/Ba/Al_2O_3 component, for which segregation of the Pt and Ba can occur during aging, migration and sintering of Pt in the Pt/CeO_2(-ZrO_2) component does not lead to the same degree of segregation, i.e., the Pt and CeO_2(-ZrO_2) remain in intimate contact, which should be beneficial for the retention of NO_x storage efficiency, as well as efficient nitrate decomposition.

(iii) Ceria-containing catalysts exhibit superior sulfation and desulfation characteristics as compared to their non-ceria analogs; more particularly, the ability of ceria to trap sulfur results in decreased sulfur accumulation on the main Ba NO_x storage component. Further, the ceria can be completely desulfated, unlike the Ba phase on which sulfur accumulation is observed over the course of repeated sulfation-desulfation cycles.

3.10 References

1. L. Cumaranatunge, S.S. Mulla, A. Yezerets, N.W. Currier, W.N. Delgass, F.H. Ribeiro, J. Catal. 246 (2007) 29.
2. J. Theis, J. Ura, C. Goralski Jr., H. Jen, E. Thanasiu, Y. Graves, A. Takami, H. Yamada, S. Miyoshi, Society of Automotive Engineers 2003-01-1160.
3. A. Desikusumastuti, T. Staudt, H. Gronbeck, J. Libuda, J. Catal. 255 (2008) 127.
4. Y. Ji, T. J. Toops, U. M. Graham, G. Jacobs, M. Crocker, Catal. Lett. 110 (2006) 29.
5. A. Yu. Stakheev, P. Gabrielsson, I. Gekas, N.S. Teleguina, G.O. Bragina, N.N. Tolkachev, G. N. Baeva, Top. Catal. 42-43 (2007) 143.
6. I. Nova, L. Lietti, L. Castolid, E. Tronconi, P. Forzatti, J. Catal. 239 (2006) 244.

7. L. Xu, R. McCabe, W. Ruona, G. Cavataio, SAE Technical Paper Series 2009-01-0285 (2009).
8. L. Olsson, H. Persson, E. Fridell, M. Skoglundh, B. Andersson, J. Phys. Chem. B 105 (2001) 6895.
9. H. Mahzoul, J.F. Brilhac, P. Gilot, Appl. Catal. B 20 (1999) 47
10. I. Nova, L. Lietti, L. Castoldi, E. Tronconi, P. Forzatti, J. Catal. 239 (2006) 244.
11. J.M. Coronado, J.A. Anderson, J. Mol.Catal. A: Chem 138 (1998) 83.
12. L. Olsson, H. Persson, E. Fridell, M. Skoglundh, B. Andersson, J. Phys. Chem. 105 (2001) 6895.
13. N.W. Cant, I.O.Y. Liu, M.J. Patterson, J. Catal. 243 (2006) 309.
14. R. Büchel, R. Strobel, F. Krumeich, A. Baiker, S.E. Pratsinis, J. Catal. 261 (2009) 201.
15. A. Kumar, M.P. Harold, V. Balakotaiah, J. Catal. 270 (2010) 214.

4. Technology Transfer

4.1 Publications

1) Y. Ji, T.J. Toops, U.M. Graham, G. Jacobs and M. Crocker, "A kinetic and DRIFTS study of supported Pt catalysts for NO oxidation", *Catal. Lett*. **110** (2006) 29.

2) Y. Ji, T.J. Toops, M. Crocker, "Effect of Ceria on the Storage and Regeneration Behavior of a Model Lean NO_x Trap Catalyst", *Catal. Lett*. 119 (2007) 257.

3) Y. Ji, J.-S. Choi, T.J. Toops, M. Crocker, M. Naseri, "Influence of ceria on the NO_x storage/reduction behavior of lean NO_x trap catalysts", *Catal. Today* 136(1-2) (2008) 146.

4) Y. Ji, T.J. Toops and M. Crocker, "Effect of Ceria on the Sulfation and Desulfation Characteristics of a Model Lean NO_x Trap Catalyst", *Catal. Lett*. 127 (2009) 55.

5) Y. Ji, T.J. Toops, J.A. Pihl, M. Crocker, " NOx storage and reduction in model lean NOx trap catalysts studied by in situ DRIFTS", *Appl. Catal. B* 91 (2009) 329.

6) Y. Ji, C. Fisk, V. Easterling, U. Graham, A. Poole, M. Crocker, J.-S. Choi, W.P. Partridge, K. Wilson, "NOx storage-reduction characteristics of Ba-based lean NOx trap catalysts subjected to simulated road aging", *Catal. Today* 151 (2010) 362.

7) V. Easterling, Y. Ji, M. Crocker, J. Ura, J.R. Theis, R.W. McCabe, "Effect of ceria on the desulfation characteristics of model lean NOx trap catalysts", *Catal. Today* 151 (2010) 338.

8) Y. Ji, V. Easterling, U. Graham, C. Fisk, M. Crocker, J.-S. Choi, "Effect of aging on the NOx storage and regeneration characteristics of fully formulated lean NOx trap Catalysts", submitted to Appl. Catal. B.

4.2 Presentations

1) Y. Ji, T.J. Toops, U.M. Graham, G. Jacobs and M. Crocker, "A kinetic and DRIFTS study of supported Pt catalysts for NO oxidation", 9th Cross-Cut Lean Exhaust Emissions Reduction Simulation (CLEERS) Workshop, Dearborn, MI, May 3-4, 2006 (poster).

2) Y. Ji, T.J. Toops and M. Crocker, "Effect of Ceria Addition on the Regeneration of a Model LNT Catalyst", Southeastern Catalysis Society Fall Symposium, Asheville, NC, September 18, 2006 (poster).

3) Y. Ji, T.J. Toops, J.-S. Choi, M. Crocker, "The Effect of CeO_2 on the Performance of Lean NOx Trap Catalysts", 10th Cross-Cut Lean Exhaust Emissions Reduction Simulation (CLEERS) Workshop, Dearborn, MI, May 1-3, 2007 (oral presentation).

4) Y. Ji, T.J. Toops, J.-S. Choi, M. Crocker, "Investigation of Aging Mechanisms in Lean NO_x Trap Catalysts", 1st Annual DOE Semi-Mega Merit Review Meeting, Crystal City, VA, June 18-19, 2007.

5) Y. Ji, T.J. Toops, J.-S. Choi, M. Crocker, "Effect of CeO_2 on the Storage and Regeneration Behavior of Lean NOx Traps", 20th North American Catalysis Society Meeting, Houston, TX, June 17-22, 2007, paper O-S4-41 (oral presentation).

6) Y. Ji, T.J. Toops, J.-S. Choi, M. Crocker, "Composition-Activity Relationships in Lean NO_x Trap Catalysts", Europacat VIII, Turku, Finland, August 26-30, 2007, paper P14-9 (poster).

7) Y. Ji, T.J. Toops and M. Crocker, "Effect of Ceria Addition on the Regeneration of a Model LNT Catalyst", Tri-State Catalysis Society Fall Symposium, Lexington, KY, November 19, 2007 (poster).

8) M. Crocker, "Investigation of Aging Mechanisms in Lean NOx Traps", Office of Vehicle Technologies 2008 Annual Merit Review Meeting, Bethseda, MD, February 25-28, 2008.

9) Y. Ji, V. Easterling, M. Crocker, T.J. Toops, J. Theis, J. Ura, R.W. McCabe, "Effect of Ceria on the Sulfation and Desulfation Characteristics of Lean NO_x Trap Catalysts", 11th Cross-Cut Lean Exhaust Emissions Reduction Simulation (CLEERS) Workshop, Dearborn, MI, May 13-15, 2008 (oral presentation).

10) Y. Ji, V. Easterling, M. Crocker, T.J. Toops, J. Theis, J. Ura, R.W. McCabe, "Effect of ceria on the sulfation and desulfation characteristics of lean NOx trap catalysts", 5th International Conference on Environmental Catalysis, Belfast, August 31-September 3, 2008, poster 181.

11) V. Easterling, J. Ura, J. Theis, R.W. McCabe, M. Crocker, "Effect of Ceria on the Desulfation Characteristics of Model Lean NOx Trap Catalysts", Tri-State Catalysis Society annual symposium, Lexington, KY, April 20, 2009 (poster).

12) M. Crocker and Y. Ji, "NOx Storage-Reduction Characteristics of Lean NOx Trap Catalysts Subjected to Simulated Road Aging", 12th Cross-Cut Lean Exhaust Emissions Reduction Simulation (CLEERS) Workshop, Dearborn, MI, April 28-30, 2009 (oral presentation).

13) M. Crocker, "Investigation of Aging Mechanisms in Lean NOx Traps", Office of Vehicle Technologies 2009 Annual Merit Review Meeting, Crystal City, VA, May 18-21, 2009.

14) Vencon Easterling, Mark Crocker, Justin Ura, Joseph Theis, Robert McCabe, "Effect of Ceria on the Desulfation Characteristics of Model Lean NO_x Trap Catalysts", paper presented at the 21st North American Catalysis Society Meeting, San Francisco, CA, June 7-11, 2009, paper P-M-18.

15) Yaying Ji, Courtney Fisk, Vence Easterling, Mark Crocker, Jae-Soon Choi, William Partridge, "NO_x Storage-Reduction Characteristics of Ba-Based Lean NO_x Trap Catalysts Subjected to Simulated Road Aging", paper presented at the 21st North American Catalysis Society Meeting, San Francisco, CA, June 7-11, 2009, paper OB19.

16) Y. Ji, V. Easterling, C. Fisk, U. Graham, M. Crocker, J.-S. Choi, "Effect of ceria on the aging characteristics of fully formulated lean NOx trap catalysts", 13th Cross-Cut Lean Exhaust Emissions Reduction Simulation (CLEERS) Workshop, Dearborn, MI, April 20-22, 2010 (poster).

17) V.G. Easterling, Y. Ji, M. Crocker, J. Ura, J.R. Theis, R.W. McCabe, "Effect of Ceria on the Desulfation Characteristics of Model Lean NOx Trap Catalysts", Tri-State Catalysis Society annual symposium, Covington, KY, April 26, 2010 (oral presentation).

18) Y. Ji, V.G. Easterling, C. Fisk, M. Crocker, J.-S. Choi , "Effect of Ceria on the Aging Characteristics of Fully Formulated Lean NOx Trap Catalysts", Tri-State Catalysis Society annual symposium, Covington, KY, April 26, 2010 (oral presentation).

19) J. Wang, Y. Ji, M. Crocker, "NOx Reduction Performance on Fresh and Aged $Pt/Ph/Ba/Al_2O_3$ Monolithic Lean NOx Trap Catalysts", Tri-State Catalysis Society annual symposium, Covington, KY, April 26, 2010 (poster).

4.3 Web sites

A description of the project has been posted on the University of Kentucky Center for Applied Energy (UK CAER) web site for the duration of the project; this description is currently available at: http://www.caer.uky.edu/factsheets/completed-projects/biofuels_crocker_LNT12-1-07.pdf

4.4 Collaborations fostered

As a consequence of the participation of Ford Motor Co., the student working on this project (Vence Easterling) was able to spend a total of 11 months at the Ford Research and Innovation Center in Dearborn, MI, where he collected data using the unique reactor facilities available there. This collaboration was further enhanced when, in February 2008, Ford awarded the UK CAER a three-year University Research Program grant, which is being used to extend this work.